Transient currents in electrolyte displacement by asymmetric electro-osmosis and determination of surface zeta potentials of composite microchannels

Ang-Tsung Kuo,[1] Chien-Hsiang Chang,[1] and Hsien-Hung Wei[1,2,a)]
[1]*Department of Chemical Engineering, National Cheng Kung University, Tainan 701, Taiwan*
[2]*Center for Micro/Nano Science and Technology, National Cheng Kung University, Tainan 701, Taiwan*

(Received 5 March 2008; accepted 3 May 2008; published online 17 June 2008)

In this article, we demonstrate the determination of surface zeta potentials of composite microchannels using the electric-field-driven solution displacement method. Nonuniform surface charge creates linear electro-osmotic flow, which leads to asymmetric displacement. Simplified circuit models are derived to determine the surface zeta potentials through examining the behavior of transient currents during the displacement. The effects of dispersion on the measured zeta potentials are discussed in line with the flow characteristics under different surface charge conditions. © *2008 American Institute of Physics*. [DOI: 10.1063/1.2936297]

As a charged surface is brought in contact with an electrolyte solution, a thin electric double layer (DL) of thickness $\lambda = 10-100$ nm is created adjacent to the surface. Due to persistent Poisson–Boltzmann equilibrium of the DL charges, the surface charge will be screened by the DL, which leads to a precipitous drop of the electric potential from the surface toward the bulk, called *zeta potential* ζ. Since $\zeta \approx \lambda \sigma_{es}/\varepsilon$ depends on the constituents of the surface and the ionic strength of the electrolyte, where σ_{es} is the surface charge density and ε is the permittivity of the electrolyte, it can reflect part of the characteristics of the surface, providing a unique fingerprint for a given surface-fluid system.

It is therefore essential to characterize surface properties through measuring the zeta potentials. The common strategy to measure the zeta potential for a charged surface is to invoke electro-osmosis (EO) by utilizing its plug flow character with the Smoluchowski slip velocity: $U = -\varepsilon \zeta E/\eta$, where E is the applied electric field and η is the viscosity of the fluid. Since U is proportional to ζ but independent of macroscopic length scales, this character offers a convenient way to determine the surface zeta potentials macroscopically by simply measuring the mobility $\mu = \varepsilon \zeta/\eta$ of the flow. While a number of techniques have been developed along this line, we in particular emphasize the transient current method[1] because it is easily implemented and capable of obtaining surface zeta potentials accurately. In this method, under the actions of EO, one electrolyte solution is displaced in a capillary by the second but with different concentrations. Since this EO-driven solution displacement renders a progressive change in the Ohmic resistance across the capillary and a transient current must respond to that change, surface zeta potentials can then be determined from the temporal behavior of the current during the displacement.

Compared to other methods,[2,3] monitoring transient currents appears more advantageous in determining zeta potentials in microsystems since it invokes neither hydrodynamic forces nor flow visualization. Moreover, given that practical microdevices are often composed of different surfaces, the current monitoring method is more appealing in measuring the zeta potentials simultaneously in such systems. It might also offer an alternative for the characterization of surfaces or assessment of interfacial kinetics.

In this article, we extend the current monitoring method to measure the zeta potentials of composite microchannels by examining the behavior of transient currents therein. We first develop equivalent circuit models to characterize the behavior of transient currents and then apply them to determine surface zeta potentials. Consider an electrolyte solution in a microchannel of length L having different charged surfaces on its top and bottom. When a linear EO is set out by the two surface velocities under an applied field, the concentration front, the invisible interface that separates the two solutions, will be immediately stretched by the shearing motion due to the velocity mismatch between the two surfaces, creating a nonuniform conductivity zone moving with the flow. As a result, instead of being perpendicular to the direction of the flow, the front will advance obliquely with respect to the flow, leading to asymmetric displacement. If the front is advected mostly by the flow without being significantly dispersed by diffusion, it will remain sharp throughout the displacement, just like a moving "slant" slicing through the two solutions in between.

The nonuniformity of solution conductivity created by asymmetric displacement immediately admits a *hybrid* Ohmic resistance in the slant zone, as it can be thought of containing two distinct conducting sheets separated by the skewed concentration front. Since the slant zone is stretched at different rates by the top and bottom surface velocities U_1 and U_2, how the resistance varies with positions will depend on the directions of these velocities, and hence on the charge attributes of the surfaces. Therefore, we consider two cases: (i) like-charge surfaces, corresponding to cocurrent displacement [Fig. 1(a)], and (ii) surfaces with opposite charges, corresponding to countercurrent displacement [Fig. 1(b)].

Let σ_1 and σ_2 stand for the conductivities of solutions 1 and 2 respectively. Also, let solution 1 be the displaced phase. For case (i), as depicted in Fig. 1(a), parallel displacement by the two different surface velocities leads the equivalent circuit to contain three resistors in series. That is, the two bulk resistances R_1 and R_2 are connected to the hybrid one R_{mix} in between, yielding the total resistance

a)Author to whom correspondence should be addressed. Electronic mail: hhwei@mail.ncku.edu.tw.

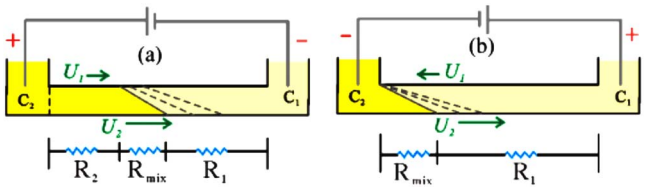

FIG. 1. (Color online) Schematic of asymmetric displacements in composite channels with (a) like-charge surfaces and (b) unlike-charge surfaces.

$R=R_1+R_{\mathrm{mix}}+R_2$. By the definition of Ohmic resistor, $R_1=(L-U_2t)/(\sigma_1 A)$ and $R_2=U_1t/(\sigma_2 A)$ with time t and the cross sectional area A of the channel. Similarly, R_{mix} can be written in terms of the apparent conductivity σ_{mix} of the slant zone: $R_{\mathrm{mix}}=(U_2-U_1)t/(\sigma_{\mathrm{mix}}A)$. Here, we approximate σ_{mix} as the *mixing-cup* average of the two conductivities: $\sigma_{\mathrm{mix}}=r\sigma_1+(1-r)\ \sigma_2$, where $r=(U_2-U_{\mathrm{av}})/(U_2-U_1)$ is the volume ratio of solution 1 occupied in the zone moving with the average velocity U_{av}. It can also be shown analytically, by solving an EO in a three-dimensional channel, that $U_{\mathrm{av}}=(U_1+U_2)/2+(U_1-U_2)\ f$, where f is a geometric factor and is a function of the depth-to-width ratio. Lumping all of the above into R and applying Ohm's law, we arrive at the following equation describing the behavior of the transient current I during $t\leqslant\tau$ (the displacement time)

$$Y\equiv\frac{I^{-1}-I_1^{-1}}{I_2^{-1}-I_1^{-1}}=\frac{\Lambda(1+2f)(U_1/U_2)+(1-2f)}{(1-2f)+(1+2f)\Lambda}\left(\frac{U_2t}{L}\right). \quad (1)$$

Here, $I_k=\Delta V/R_k$ is the current under voltage ΔV across the channel when the channel is completely filled by solution k ($k=1,2$), and $\Lambda=\sigma_1/\sigma_2$ is the conductivity ratio. Also, instead of using current as in the usual methodology, we take inverse current as our primary variable to reflect the linear change in the resistance with time. In the special case with $U_1=U_2\equiv U$, Eq. (1) reduces to $(I^{-1}-I_1^{-1})/(I_2^{-1}-I_1^{-1})=Ut/L$, in accordance with the usual recipe using uniformly charged channels.[1]

For unlike-charge case, in which the two surface velocities are in the opposite directions, however, the displacement process, as depicted in Fig. 1(b), differs from that in like-charge case. Suppose that the displacing phase (solution 2) starts from the left and flows toward the right. Because of the opposition between the two surface velocities, the displaced phase (solution 1) near the upper left portion of the channel will be entrained by the top surface velocity and flows back to the left reservoir. On the other hand, the nearby displacing phase is discharged from the same reservoir due to the bottom surface velocity. Such counteraction between the local fluid entrainment and discharge makes the fluid near the left corner virtually stationary. Thereby, one end of the concentration front can be thought of being pinned at the left corner while the other is pulled by the bottom surface and advances toward the right. As a result, the slant zone is stretched mostly by the bottom velocity U_2 and hence, the equivalent circuit is constituted merely by R_{mix} and R_1 in series. The mixing-cup conductivity of the slant zone now becomes $\sigma_{\mathrm{mix}}=(1-U_{\mathrm{av}}/U_2)\ \sigma_1+(U_{\mathrm{av}}/U_2)\sigma_2$. Following the similar procedure in deriving Eq. (1), we derive the transient current for countercurrent displacement

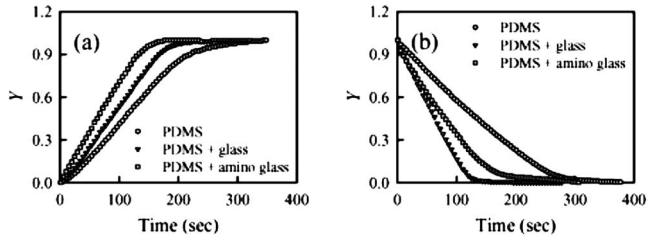

FIG. 2. Temporal responses of normalized inverse transient currents. The results are obtained by displacing (a) the higher conductivity and (b) the lower conductivity solutions, respectively.

$$Y=\frac{(1+2f)(U_1/U_2)+(1-2f)}{(1-\Lambda)(1+2f)(U_1/U_2)+(1-2f)+(1+2f)\Lambda}\left(\frac{U_2t}{L}\right). \quad (2)$$

Note here that $-1<U_1/U_2<0$.

As indicated by Eqs. (1) and (2), transient currents in composite channels behave like that conveyed by the effective EO velocity βU_2 in an analogous uniformly charged channel, where β is the prefactor of (U_2t/L) in these equations. It is also worth noting that when the two conductivities are nearly matched, i.e., $\Lambda\approx 1$, both Eqs. (1) and (2) take the approximate form: $(I^{-1}-I_1^{-1})/(I_2^{-1}-I_1^{-1})\approx U_{\mathrm{av}}t/L$, regardless of the direction of the displacement. In this limit, $\beta U_2\approx U_{\mathrm{av}}$ and the displacement is simply carried out by the average fluid velocity. Our model equations are applicable to convection-dominant displacement. The justification of our approach is given in Ref. 4.

We examine electrolyte displacement in PDMS channels, which carry negative charge, on the following substrates: (i) PDMS, (ii) bare glass with negative charge, and (iii) amino-coated glass with positive charge,[5] representing uniformly charged, like-charge, and unlike-charge systems, respectively. The experiments were conducted by following the procedures similar to Ref. 1, and the details can be found in Ref. 4. Representative transient currents are plotted in terms of normalized inverse current Y and shown in Fig. 2. The zeta potentials can be readily obtained from the slopes of these curves. In Fig. 2(a), the lower conductivity solution displaces the higher one, giving rise to an increase in the resistance with time. The results reveal that it takes shorter time to complete displacement in PDMS-glass composite channels compared to that in a uniform PDMS channel, suggesting that the magnitudes of the zeta potentials of the glasses must be larger than that of PDMS. Indeed, the measured zeta potentials for PDMS, bare glass, and amino-coated glass are -19.4 ± 4.7, -27.1 ± 15.2, and 133.7 ± 20.5 mV, respectively.[6] Figure 2(b) shows similar results obtained by displacing the lower conductivity solution, as evidenced by a decrease in the resistance with time. The corresponding zeta potentials for PDMS, bare glass, and amino-coated glass are -17.2 ± 5.0, -47.5 ± 18.6 and 90.6 ± 13.1 mV. Comparing these two sets of the data, first of all, we find that for a PDMS channel the measured zeta potentials do not exhibit an apparent disparity as reversing the flow, as a uniform EO does not cause any hydrodynamic dispersion.[4] These data also agree well with the reported value of -19.1 mV obtained by different techniques,[6] verifying the reliability of our approach. The variations of the data could arise from additional dispersion induced by the pre-existing conductivity difference.[4]

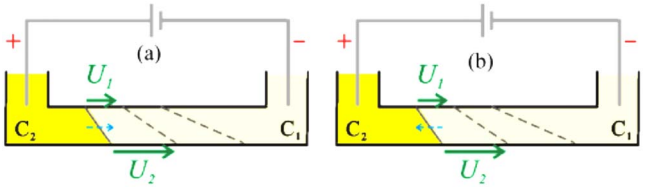

FIG. 3. (Color online) Illustration of the effects of axial dispersion (dashed arrows) on the concentration front in a composite channel with like-charge surfaces. Displacement is toward the right. (a) $C_2 > C_1$ and (b) $C_2 < C_1$.

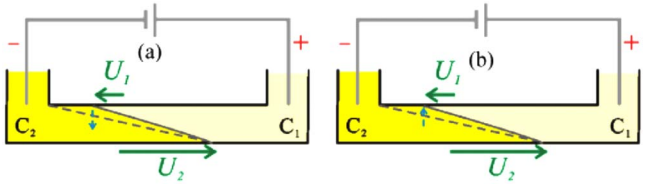

FIG. 4. (Color online) Illustration of the effects of transverse dispersion (dashed arrows) due to the overstretched concentration front in a composite channel with opposite charge surfaces. Displacement is toward the right. (a) $C_2 < C_1$ and (b) $C_2 > C_1$.

For composite cases, however, because dispersion can either assist or oppose the displacement, the measured zeta potentials of the glasses exhibit apparent differences when reversing displacement directions. In addition, the relative variations of the data appear larger than those in pure PDMS case because hydrodynamic dispersion can now be induced by both shear flow and conductivity gradient.[4] Nevertheless, since dispersion contributes a few tens percent of variations in typical zeta potential measurements, we conclude that the displacement process is dominated by convection, and hence the transient current, as described by our circuit model Eq. (1) or (2). Below, we explain how dispersion effects cause the observed discrepancies of the data between the two displacement directions.

For the PDMS channel on a bare glass substrate, cocurrent surface flows with different velocities are produced by the two like-charge surfaces, shearing the fluid, and hence stretching the concentration front during the displacement. Note that the leading edge of the concentration front is located on the glass side because of higher surface charge than PDMS. In this case, we observe that the magnitude of the measured zeta potential of the glass is larger when displacing the lower conductivity solution. Because axial diffusion set by the two solutions acts in the same direction as convection [Fig. 3(a)], this reinforces solute transport, making the leading edge extended more toward the lower conductivity end. As a result, the dispersed concentration front looks like gaining a speed and hence overestimates the zeta potential. Similarly, by displacing the higher conductivity solution, axial diffusion is now opposed by the flow [Fig. 3(b)] and thus, the surface zeta potential should appear smaller in magnitude as measured. Nevertheless, our measured value for either case shows reasonable agreement with the reported −30.1 mV.[6]

As for the PDMS channel on an amino-coated glass substrate, the two surfaces now have opposite charges. In this scenario, as described in Fig. 1(b), because the zeta potential of the glass is higher than that of the PDMS in magnitude, the leading edge of the concentration front advances along the glass surface while the other end is virtually pinned at the PDMS surface. The measured glass zeta potential, in contrast to like-charge case, appears higher (lower) in the displacement toward the higher (lower) conductivity end. As illustrated in Fig. 4, because the concentration front is now sheared by the two opposite surface flows and advected at a much higher speed, the front would become so extended that the solutions are laminated into two layers penetrating each other. This overstretched front in turn creates large concentration gradients across the channel depth, making the front more susceptible to being dispersed in the transverse direction than in the axial direction.[4] Such transverse dispersion is the strongest near the pinned end where the flow is the slowest but diminishes away from it because of the gradual increase in axial convection. As a result, the dispersed region will be enriched by the higher conductivity phase. This enrichment in turn increases (decreases) the apparent conductivity when displacing higher (lower) conductivity solution, and hence, the displacement speed, resulting in the larger (smaller) magnitude of the measured zeta potential.

To our best knowledge, the present work is the first demonstration of measuring surface zeta potentials of composite channels using the current monitoring method. We show that the behavior of the transient currents in composite microchannels differs from that in uniformly charged channels due to asymmetric displacement arising from the nonuniform EO. Also, because of hydrodynamic dispersion and its interplay with the EO, transient currents can show different responses when reversing the displacement direction, and hence, affect the zeta potential measurement. While surface zeta potentials can be measured with satisfactory accuracy by using our simple dispersion-free circuit models, more reliable measurement requires a more rigorous approach to account for hydrodynamic dispersion. One can, in principle, obtain the conductivity distribution by solving a cross-sectional averaged convective-diffusion equation whose effective dispersion coefficient is a function of the unknown zeta potentials. The responded transient current can then be derived in terms of the averaged resistance across the channel length for finding the zeta potentials. Prior to such a detailed analysis (which is beyond the scope of this work), the present work is nevertheless an *ab initio* attempt that provides some insight into the phenomenon. Hence, it can serve as a useful guidance for conducting more accurate measurement of surface zeta potentials of practical microdevices.

This work was supported by the National Science Council of Taiwan under Grant Nos. NSC95-2221-E-006-309 of C.H.C. and NSC 96-2628-E-006-077 of H.H.W.

[1]X. Huang, M. J. Gordon, and R. N. Zare, Anal. Chem. **60**, 1837 (1988); L. Ren, J. Masliyah, and D. Li, J. Colloid Interface Sci. **257**, 85 (2003).
[2]S. L. Walker, S. Bhattacharjee, E. M. V. Hoek, and M. Elimelech, Langmuir **18**, 2193 (2002).
[3]S. Devasenathipathy and J. G. Santiago, Anal. Chem. **74**, 3704 (2002); M. H. Oddy and J. G. Santiago, J. Colloid Interface Sci. **269**, 192 (2003); D. Yan, C. Yang, N.-T. Nguyen, and X. Huang, Electrophoresis **27**, 620 (2006).
[4]See EPAPS document No. E-APPLAB-92-037821 for model validation and experimental details. For more information on EPAPS, see http://www.aip.org/pubservs/epaps.html.
[5]Z. L. Chen, F. C. Hsu, D. Battigelli, and H.-C. Chang, Anal. Chim. Acta **569**, 76 (2006).
[6]B. J. Kirby and J. E. F. Hasselbrink, J. Colloid Interface Sci. **25**, 203 (2004).